Towards Rapid Mycetoma Species Diagnosis: A Deep Learning Approach for Stain-Invariant Classification on H&E Images from Senegal

Kpêtchéhoué Merveille Santi ZINSOU[1,3 [0000−0003−0518−848X]], Cheikh Talibouya DIOP[1,3 [0000−0002−9617−5619]], Idy DIOP[2,3 [0000−0002−9143−196X]], Apostolia Tsirikoglou[4 [0000−0003−0298−937X]], Emmanuel Edwar SIDDIG[5 [0000−0001−6314−7374]], Doudou SOW[1 [0000−0002−0560−2372]], and Maodo NDIAYE[2 [0000−0001−5812−2770]]

[1] University of Gaston Berger (UGB), BP: 234 Saint-Louis, SENEGAL
{zinsou.kpetchehoue-merveille-santi,cheikh-talibouya.diop}@ugb.edu.sn
[2] University Cheikh Anta Diop, Dakar, SENEGAL
[3] UMMISCO SENEGAL, Institut de Recherche pour le Développement (IRD)
[4] Karolinska Institutet, SWEDEN
[5] University of khartoum, SUDAN

Abstract. Mycetoma, categorized as a Neglected Tropical Disease (NTD), poses significant health, social, and economic challenges due to its causative agents, which include both bacterial and fungal pathogens. Accurate identification of the mycetoma type and species is crucial for initiating appropriate medical interventions, as treatment strategies vary widely. Although several diagnostic tools have been developed over time, histopathology remains a most used method due to its quickness, cost-effectiveness and simplicity. However, its reliance on expert pathologists to perform the diagnostic procedure and accurately interpret the result, particularly in resource-limited settings. Additionally, pathologists face the challenge of stain variability during the histopathological analyses on slides. In response to this need, this study pioneers an automated approach to mycetoma species identification using histopathological images from black skin patients in Senegal. Integrating various stain normalization techniques such as macenko, vahadane, and Reinhard to mitigate color variations, we combine these methods with the MONAI framework alongside DenseNet121 architecture. Our system achieves an average accuracy of 99.34%, 94.06%, 94.45% respectively on Macenko, Reinhard and Vahadane datasets. The system is trained using an original dataset comprising histopathological images stained with Hematoxylin and Eosin (H&E), meticulously collected, annotated, and labeled from various hospitals across Senegal. This study represents a significant advancement in the field of mycetoma diagnosis, offering a reliable and efficient solution that can facilitate timely and accurate species identification, particularly in endemic regions like Senegal.

Keywords: Mycetoma · Histopatology · Deep learning · Senegal · Mycetoma species · CNN · black skin · stain normalization.

1 Introduction

Mycetoma (Fig 1), a chronic infection characterized by the slow evolution over months or years, presents a significant challenge due to its progressive extension and destruction of muscle, tendon, fascia, and bone. This condition manifests through a distinctive triad of symptoms: a painless subcutaneous mass, multiple fistulae, and discharge containing granules, caused by either bacterial (actinomycetoma) or fungal (eumycetoma) agents whose in vivo form of development is grain [1]. Originating from soil and plant saprophytes, particularly in rural environments, mycetoma primarily affects males within the 20-40 age group [2], predominantly in tropical and subtropical regions known as the "mycetoma belt" [3]. Despite its endemic nature, precise data on its incidence and prevalence remain scarce. Senegal, within this belt, serves as a focal point for studying mycetoma. A study by Aida-Sadikh Badiane and al. [4] investigated mycetoma prevalence in Senegal and revealed 338 diagnosed cases between 1993 and 2016. Another study [5] reported 193 diagnosed cases in Senegal between 2008 and 2018. Additionally, Wendy W. and al. [6] identified the most prevalent mycetoma species in Senegal as Madurella mycetomatis, Streptomyces somaliensis, Actinomadurea pelletieri, and Actinomadurea madurea.

Recognized as a neglected tropical disease by the World Health Organization [3], mycetoma presents significant challenges in diagnosis, management, and understanding. Delayed detection of mycetoma often necessitates limb amputation, highlighting the crucial need for early and accurate diagnosis. This is critical as treatment approaches differ significantly, impacting therapeutic outcomes. The diagnostic landscape in dermatology, particularly concerning on "black skin," confronts substantial obstacles due to a shortage of dermatologists with specialized training for this demographic, compounded by the inherent complexities of interpreting skin conditions on black skin[7]. In rural areas, limited healthcare infrastructure and pathologist expertise exacerbate these challenges, resulting in inadequate resources for patient care.

Over time, a plethora of techniques and tools have emerged to streamline the diagnosis of mycetoma [8–10]. Among these, histopathology stands out as the swiftest diagnostic method, although distinguishing between eumycetoma and actinomycetoma and identifying specific species pose significant challenges[11, 12]. Currently, histopathological diagnosis relies heavily on skilled pathologists for accurate and timely assessments. Each mycetoma species presents distinctive grain characteristics, sizes, colors, and patterns, adding layers of complexity to interpretation, particularly with histochemical staining. Microscopic examination of histopathological slides introduces variability among observers, prolonging and complicating the diagnostic process.

Moreover, histopathological analyzes on slides face the challenge of stain variability [13]. Indeed, the data collection process allowed us to observe color variations between slices from different patients of the same mycetoma species stained with hematoxylin and eosin (H&E). Figure 2 shows this color variation between the slides of different patients who have been diagnosed with mycetoma with the species madurella mycetomatis. These coloring discrepancies can come from various factors. First, differences in staining protocols between laboratories, and even within the same laboratory, can result in variations in intensity and staining. Secondly, variations in tissue composition, including differences in cell types and tissue structures, can influence stain

absorption, thereby altering the appearance of stained slides. Additionally, disparities in sample age, handling, and quality of reagents and staining equipment can contribute to staining variations. Technological factors, such as differences in the type of staining equipment or calibration, may further affect results. Additionally, environmental conditions such as temperature and humidity can impact coloring results. Inconsistencies in species identification and treatment delays, arising from these challenges, have a significant impact on patient outcomes. Therefore, there is a need for automated and standardized approaches to improve the accuracy and efficiency of mycetoma diagnosis from histopathological images.

Fig. 1. Mycetoma

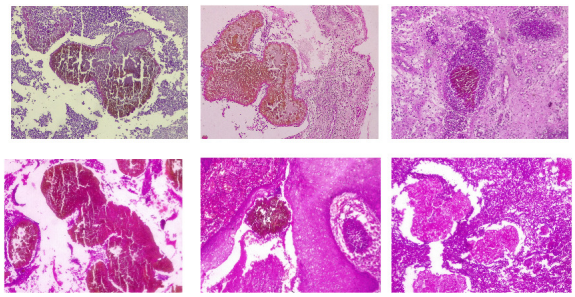

Fig. 2. Histopathological images of slices stained with H&E from six different patients showing color variation for Madurella mycetomatis species

The rise of artificial intelligence (AI) has transformed the landscape of skin disease diagnosis, surpassing human observation in accuracy. Its integration across diverse sectors has streamlined the identification, diagnosis, and treatment of skin conditions. To support histopathological diagnosis based on images, numerous deep learning and machine learning algorithms have been developed. However, a significant challenge lies in the availability of data to fuel these algorithms, particularly evident in Senegal.

In response to these challenges, our study focuses on gathering data from various hospitals to establish an original histopathological image dataset specific to Senegal. We employ various stain normalization techniques such as Macenko, Vahadane, and Reinhard to address color and intensity variations in stained images originating from different laboratories. Subsequently, we employ a combination of the MONAI framework with the DenseNet121 model to classify images into four distinct classes. Remarkably, our system achieves high accuracy in automatically identifying four prevalent mycetoma species in Senegal: *Madurella mycetomatis* (MM), *Falciformispora senegalensis* (FS), *Actinomadura pelletieri* (AP), and *Streptomyces somaliensis* (SS), as illustrated respectively in Figures (3, 4, 5, 6) Our contributions are summarized as follows:

- We gather, annotate, and label histopathological images stained with H&E from diverse hospitals to establish an original dataset specific to mycetoma in Senegal.
- We employ stain normalization techniques including Macenko, Vahadane, and Reinhard to address color and intensity variation in collected images.

– We implement a unified approach using the MONAI framework in conjunction with the DenseNet121 model for classifying images into four mycetoma species .

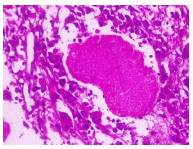

Fig. 3. MM

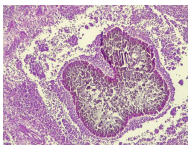

Fig. 4. FS

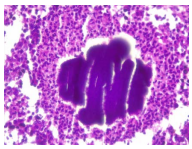

Fig. 5. AP

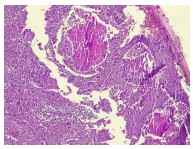

Fig. 6. SS

2 Related work

2.1 Mycetoma

Hyam Omar et al. [18, 19] introduced a computational approach achieving an accuracy of 91.8% in distinguishing between eumycetoma and actinomycetoma. Their methodology leveraged radiomics, extracting a diverse quantitative features from histopathological images converted into grayscale. Utilizing Partial Least Square Discriminant Analysis (PLS-DA), they successfully classified mycetoma types using a dataset comprising 890 images sourced from the Mycetoma Research Center in Khartoum.

While recognized as a pioneering system for mycetoma diagnosis, it is limited to distinguishing solely between eumycetoma and actinomycetoma, a point emphasized by Develoux [1], who stresses the importance of accurately identifying the species for initiating appropriate treatment. Consequently, there is a necessity to explore avenues for automating mycetoma species identification.

2.2 Stain normalization methods

Inconsistencies in staining color, can profoundly impact the accuracy of computer-aided diagnosis and pathologists' interpretations. To tackle this issue, several stain normalization techniques have been developed, significantly enhancing the accuracy, and efficiency of histopathology image analysis. In their paper, Md. Ziaul Hoque and al.[14] conducted a thorough review and experimental comparison of distinct stain color normalization methods. Their findings underscore the importance of carefully selecting the appropriate normalization technique, considering the specific application and image characteristics. Digital pathology experts must meticulously evaluate the implications of any normalization or feature extraction technique on downstream analysis, opting for the most suitable approach for the given application.

3 Methodology

This section outlines the proposed methodology, which comprises three main stages: data collection and annotation, image stain normalization, and image classification.

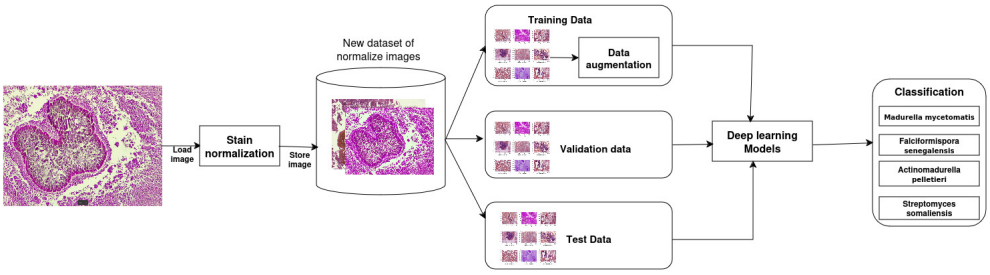

Fig. 7. The proposed system block diagram

The methodology, depicted in the figure 7, begins with the collection of data from various hospitals in Senegal to generate an original set of histopathology images. In the second step, to tackle the challenge posed by variations in stains among images depicting the same species, we utilize three distinct stain normalization techniques: Macenko, Reinhard, and Vahadane. Each normalization method is applied to the images, resulting in three separate datasets in addition to the original dataset. These datasets serve as inputs for our deep learning model, which utilizes the MONAI framework in conjunction with the DenseNet121 model to classify the four mycetoma species considered in this study. MONAI transforms are applied to process and augment the training set of each dataset. Furthermore, the model is trained on the original dataset comprising non-normalized images.

3.1 Data Collection and Annotation

Our research focuses on the Senegalese population diagnosed with mycetoma, encompassing individuals of all ages and genders. We conducted a comprehensive study utilizing histopathological images showcasing tissue reactions and granular morphology post-application of histochemical stains known as H&E (Hematoxylin and Eosin). This study incorporates data from 27 patients, 67 slices, each patient contributing between 1 to 6 tissue slices. Employing the 'Leica icc50 e' microscope, connected to a desktop monitor equipped with the Leica software, we captured multiple images from each slice, emphasizing the presence of one or several grains within the portion. Three magnification levels were employed: HI PLAN 4x/0.10 PH0, HI PLAN 10x/0.25 PH1, and HI PLAN 100x/1.25 OIL.

Following image collection, in collaboration with pathologists from Senegal and Sudan, mycetoma species were meticulously identified and annotated for each image. We obtained a total of 1289 images representing four different species as summerised in the table 1: *Madurella mycetomatis* (MM), *Falciformispora senegalensis* (FS), *Actinomadura pelletieri* (AP), and *Streptomyces somaliensis* (SS).

Table 1. Detail of the collected dataset per specie

Type	EUMYCETOMA		ACTINOMYCETOMA		
Species	**Madurella mycetomatis**	**Falciformispora senegalensis**	**Actinomadura pelletieri**	**Streptomyces somaliensis**	**Total**
Image per species	493	195	378	223	1289
Number of slices	32	14	8	10	64
Number of patient	10	06	06	05	27

3.2 Stain normalization

Given the importance of conserving tissue structure information and considering color features for the identification of myctoma species, our study focused on three methods: Macenko[15], Reinhard[16], and Vahadane[17].

Vahadane's method is notable for its capability to harmonize the color of source images with that of target images while conserving all original structures. This method employs a process of decomposing the image into sparse and non-negative stain density maps, which are subsequently merged based on the stain color of a pathologist's preferred target image. **Reinhard's method** excels in color correction by employing a transformation to align the color statistics of input images with a designated target reference image. This process preserves the structural integrity of the source image while ensuring a consistent contrast comparable to the target image. **Macenko's method** computes an optimal stain color basis to convert the color space of each image to a standardized reference, showcasing resilience to fluctuations in staining and lighting conditions. This process entails identifying distinct stain vectors for each image, which are determined based on the colors present in the image.

It is essential to emphasize that, through collaboration with pathologists, we have identified specific target images for each species. These target images will serve as references for standardizing the source images. The implementation of the three methods, as depicted in Figure 8, has resulted in the creation of three new datasets: Macenko, Reinhard, and Vahadane. To assess the performance of each stain normalization technique on individual mycetoma species, we utilized two metrics: Structural Similarity Index (SSIM) [20], which evaluates the similarity between the normalized image and the source image by comparing the structural information rather than just pixel values, and Peak Signal-to-Noise Ratio (PSNR) [21], which measures the quality of an image by comparing it to a reference image. As depicted in Figure 9, showcasing the metrics of various images generated in Figure 8, it becomes apparent that the Reinhard method yields superior scores, followed by Macenko and Vahadane, in terms of the SSIM metric. Conversely, for the PSNR metric, Vahadane demonstrates the best performance, followed by Macenko and Reinhard. Notably, it is observed that the ranking of these methods varies depending on each species, indicating a significant enhancement in reducing color variability among images while preserving the structure of the source images.

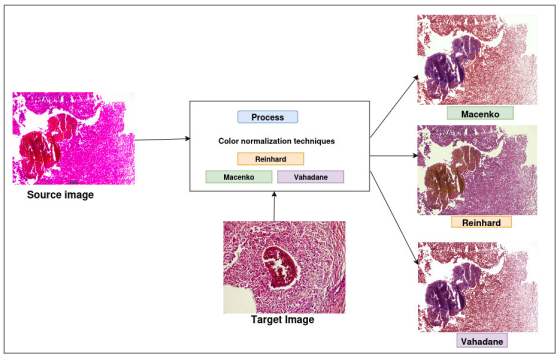

Fig. 8. Color normalization process with Macenko, Reinhard and Vahadane techniques

Methods	SSIM source	PSNR source
Reinhard	0.868381	13.104665
Vahadane	0.782268	13.180122
macenko	0.812106	13.883441

Fig. 9. SSIM and PSNR metric evaluation

3.3 MONAI framework with DenseNet121

The MONAI framework [22], acronym for Medical Open Network for AI, is designed to address medical imaging tasks, providing a specialized toolkit tailored for medical image analysis challenges. In our study, we leveraged MONAI transforms to preprocess and enhance mycetoma images, seamlessly integrating them with deep learning models to facilitate precise and robust analysis. By applying various data augmentation techniques such as random rotation, flipping, zooming, and resizing, we standardized each image to a consistent size of 300x300 pixels exclusively within the training set of each dataset. This meticulous preprocessing strategy optimizes the data for training, thereby enhancing the model's ability to extract meaningful insights and deliver accurate diagnoses. Additionally, MONAI offers pre-implemented network architectures, including DenseNet, which served as the backbone for our image classification model. DenseNet [23] lies in dense connectivity, wherein each layer establishes direct connections with every other layer in a forward-propagating manner. It aims to address the vanishing gradient issue and promote feature reuse across the network.

4 Experiments and results

4.1 Implementations details

The system is constructed using the PyTorch framework (version: 2.1.0+cu121) and incorporates the MONAI framework (version: 1.4.dev2407). Training was carried out on a T4 GPU within the Google Colab environment.

Following the application of three stain normalization methods, we obtained four distinct datasets: original, Macenko, Reinhard, and Vahadane. To comprehensively assess the model's performance, a stratified 4-fold cross-validation [24] method was adopted to enhance its robustness across various training and test sets. This approach involves splitting the data into K folds while ensuring that each fold maintains the same class label proportions as the original dataset. Consequently, each stained and

original dataset is randomly divided into four separate training (80%) and test sets (20%), ensuring equitable patient distribution in each set. Additionally, 15% of the images are randomly set aside from each training set for validation, without overlap, and are utilized for parameter selection. This partitioning results in each dataset being divided into training (70%), validation (10%), and test (20%) sets. Such partitioning ensures that data from the same patient are not present in both the training and test sets, thereby preserving data integrity. These partitioned datasets serve as inputs for our deep learning model, which leverages the MONAI framework alongside the DenseNet121 model to classify the four mycetoma species considered in this study.

All images were resized to 300x300, and MONAI transforms were employed to process and augment (including random rotation, random flip, and random zoom) the training set of each dataset. For training, the CrossEntropyLoss function was utilized over 15 epochs with a batch size of 32. The Adam optimizer was employed with a base learning rate of 1e-5 across all experiments, and the DenseNet from MONAI was used for classification. Evaluation was performed using the accuracy, precision, recall and f1-score metrics.

4.2 Results

The MONAI framework's performance, combined with DenseNet121, underwent assessment for mycetoma species identification. Table 2 presents results from cross-validation sets trained and validated using both stain-normalized and non-normalized datasets. Our model exhibited superior performance on the Macenko dataset, achieving an average accuracy of 99.34%. Furthermore, the model demonstrated similar average performance on the Reinhard and Vahadane datasets, reaching accuracies of 94.06% and 94.45%, respectively. Conversely, the same table indicates the average metrics of the non-normalized image dataset, yielding a performance of 49.01%, significantly lower than that achieved by normalization methods.

In conclusion, different normalization methods facilitate enhanced species identification compared to using images collected without normalization. The 94% accuracy obtained on the Reinhard and Vahadane datasets can be attributed to their emphasis on conserving tissue structure information, unlike the Macenko method.

5 Conclusion

This study introduces an innovative method for automatically identifying four prevalent mycetoma species in Senegal with remarkable accuracy. Through the utilization of color normalization techniques such as Macenko, Vahadane, and Reinhard, we effectively addressed stain variations in histopathology images, which are critical for precise species identification. Furthermore, by retaining color features with the use of color images, we employed the MONAI framework and DenseNet121 to achieve efficient species classification. Although this study focused on a relatively small cohort of 27 patients, there are promising avenues for future research. These include expanding the system's identification capabilities to encompass additional mycetoma

Table 2. Model Performance Evaluation on Each Dataset

Dataset	Metrics	1st Fold	2nd Fold	3rd Fold	4th Fold	Average
Macenko	**Accuracy**	0.9850	0.9964	1.00	0.9922	**0.9934**
	Precision	0.9787	0.9949	1.00	0.9904	**0.991**
	Recall	0.9867	0.9954	1.00	0.9912	**0.993325**
	F1-Score	0.9821	0.9951	1.00	0.9908	**0.992**
Reinhard	**Accuracy**	0.9662	0.9312	0.9591	0.9059	**0.9406**
	Precision	0.9817	0.9594	0.9763	0.9478	**0.9663**
	Recall	0.9477	0.9120	0.9329	0.8537	**0.911575**
	F1-Score	0.9613	0.9245	0.9488	0.8674	**0.9255**
Vahadane	**Accuracy**	0.8947	0.9457	0.9926	0.9451	**0.944525**
	Precision	0.8797	0.9668	0.9948	0.9386	**0.944975**
	Recall	0.8988	0.9306	0.9915	0.9381	**0.93975**
	F1-Score	0.8885	0.9419	0.9931	0.9383	**0.94045**
Original Data Not Normalized	**Accuracy**	0.5038	0.7246	0.3383	0.3937	**0.4901**
	Precision	0.5237	0.8115	0.3002	0.3305	**0.491475**
	Recall	0.5165	0.6778	0.2755	0.3391	**0.452225**
	F1-Score	0.4903	0.7012	0.2794	0.3299	**0.4502**

species and improving model generalization through the collection of larger datasets involving a greater number of patients. These advancements hold the potential to significantly enhance the system's performance and contribute to a deeper understanding and management of mycetoma.

Acknowledgments. The authors are thankful for the support provided by the Regional Scholarship and Innovation Fund (RSIF), and the Partnerships for Skills in Applied Sciences, Engineering, and Technologies (PASET).
We extend our sincere gratitude to Dr. Abdou Magib Gaye and Ms. Habone Ahmed Mahamoud for their invaluable assistance in collecting histopathology slide samples.

Funding. This work was supported by the Regional Scholarship and Innovation Fund (RSIF), and the Partnerships for Skills in Applied Sciences, Engineering, and Tech- nologies (PASET).

Disclosure of Interests. The authors have no competing interests to declare that are relevant to the content of this article.

References

1. M.Develoux: Mycetoma and their treatment, Journal de Mycologie Médicale Volume 26, Issue 2, June 2016, Pages 77-85. https://doi.org/https://doi.org/10.1016/j.mycmed.2016.03.005
2. Dr latreche: Mycétome. Courtesy of M. McGinnis Copyright Doctorfungus Corpporation, Location(2000). https://fmedecine.univ-setif.dz/ProgrammeCours/parasito.Myc%C3%A9tome%20medeci2020.pdf
3. Organisation Mondiale de la Santé: Mycétome DERMATOLOGIE EN MILIEU TROPICAL-PDF. Last accessed 13 Oct 2022. https://www.who.int/fr/news-room/fact-sheets/detail/mycetoma
4. AidaSadikh Badiane and al.: Point sur l'épidémiologie des mycétomes au Sénégal. Journal de Mycologie Médicale, Volume 27, Issue 3, September 2017, Page e7. https://doi.org/10.1016/j.mycmed.2017.04.024

5. Sow D, Ndiaye M, Sarr L, Kanté MD, Ly F, Dioussé P, et al. (2020) Mycetoma epidemiology, diagnosis management, and outcome in three hospital centres in Senegal from 2008 to 2018. PLoS ONE 15(4): e0231871. https://doi.org/10.1371/journal.pone.0231871
6. van de Sande WWJ (2013) Global Burden of Human Mycetoma: A Systematic Review and Meta-analysis. PLoS Negl Trop Dis 7(11): e2550. https://doi.org/10.1371/journal.pntd.0002550
7. Zinsou, K.M.S., Diop, I., Diop, C.T., Bah, A., Ndiaye, M., Sow, D. (2023). Survey of Detection and Identification of Black Skin Diseases Based on Machine Learning. In: Saeed, R.A., Bakari, A.D., Sheikh, Y.H. (eds) Towards new e-Infrastructure and e-Services for Developing Countries. AFRICOMM 2022. Lecture Notes of the Institute for Computer Sciences, Social Informatics and Telecommunications Engineering, vol 499. Springer, Cham. https://doi.org/10.1007/978-3-031-34896-9_16
8. Hao, X.; Cognetti, M.;Burch-Smith, R.; Mejia, E.O.; Mirkin,G.: Mycetoma: Development of Diagnosis and Treatment. J. Fungi 2022, 8, 743. https://doi.org/ 10.3390/jof8070743
9. University of Khartoum : MYCETOMA Online training Module, https://mycetoma.edu.sd/elearning/ Last accessed 30 Sept 2022
10. Ahmed AA, van de Sande W, Fahal AH. Mycetoma laboratory diagnosis: Review article. PLoS Negl Trop Dis. 2017 Aug 24;11(8):e0005638. https://doi.org/10.1371/journal.pntd.0005638. PMID: 28837657; PMCID: PMC5570215.
11. Siddig EE, Fahal AH (2017) Histopathological Approach in Diagnosis of Mycetoma Causative Agents: A Mini Review. J Cytol Histol 8: 466. https://doi.org/ 10.4172/2157-7099.1000466
12. van de Sande WWJ, Fahal AH, Goodfellow M, Mahgoub ES, Welsh O, et al. (2014) Merits and Pitfalls of Currently Used Diagnostic Tools in Mycetoma. PLoS Negl Trop Dis 8(7): e2918. https://doi.org/10.1371/journal.pntd.0002918
13. B. Lakshmanan, S. Anand, and T. Jenitha, "Stain removal through color normalization of Haematoxylin and eosin images: areview," Journal of Physics: Conference Series, vol. 1362, no. 1, Nov. 2019, https://doi.org/10.1088/1742-6596/1362/1/012108.
14. Md. Ziaul Hoque, Anja Keskinarkaus et al.: "Stain normalization methods for histopathology image analysis: A comprehensive review and experimental comparison", Information Fusion, Volume 102, 2024, 101997, ISSN 1566-2535, https://doi.org/10.1016/j.inffus.2023.101997.
15. Marc Mackeno,Charles Schmitt.,"A Method for Normalizing Histology Slides for Quantative Analysis," IEEE International Symposium on Biomedical Imaging,pp.11071110, 2009.
16. Reinhard, E., Ashikhmin, M., Gooch, B., & Shirley, P. (2001). Color Transfer between Images. IEEE Computer Graphics and Applications, 21, 34-41.
17. Vahadane A, Peng T, Sethi A, Albarqouni S, Wang L, Baust M, Steiger K, Schlitter AM, Esposito I, Navab N. Structure-Preserving Color Normalization and Sparse Stain Separation for Histological Images. IEEE Trans Med Imaging. 2016 Aug;35(8):1962-71. https://doi.org/10.1109/TMI.2016.2529665. Epub 2016 Apr 27. PMID: 27164577.
18. Hyam Omar Ali and al. : Radiomics Model for Mycetoma Grains Classification from Histopathological Microscopic Images Using Partial Least Squares Discriminant Analysis (PLS-DA), Preprint submitted on 3 Jun 2021. https://hal.archives-ouvertes.fr/hal-03247688
19. Omar Ali Hyam et al.: "Evaluation of a computational model for mycetoma-causative agents identification." Transactions of the Royal Society of Tropical Medicine and Hygiene, trad057. 13 Dec. 2023, https://doi.org/10.1093/trstmh/trad057
20. Nilsson, Jim and Tomas Akenine-Möller. "Understanding SSIM." ArXiv abs/2006.13846 (2020): n. pag, https://doi.org/10.48550/arXiv.2006.13846.
21. A. Horé and D. Ziou, "Image Quality Metrics: PSNR vs. SSIM," 2010 20th International Conference on Pattern Recognition, Istanbul, Turkey, 2010, pp. 2366-2369, https://doi.org/10.1109/ICPR.2010.579.

22. M. Jorge Cardoso et al.: "MONAI: An open-source framework for deep learning in healthcare." , arXiv preprintarXiv:2211.02701. 2022, 4 Nov 2022, https://doi.org/10.48550/arXiv.2211.02701
23. Huang, G. et al.: Densely connected convolutional networks. In Proceedings of the IEEE conference on computer vision and pattern recognition (pp. 4700-4708), https://doi.org/10.48550/arXiv.1608.06993
24. Diamantidis, N. A., Karlis, D., & Giakoumakis, E. A. (2000). Unsupervised stratification of cross-validation for accuracy estimation. Artificial Intelligence, 116(1-2), 1–16. https://doi.org/10.1016/s0004-3702(99)00094-6